Heterogeneous Bulk Polymerization of Styrene in the Presence of Polybutadiene: Calculation of the Macromolecular Structure

Natalia Casis,[1] Diana Estenoz,[1] Luis Gugliotta,[1] Haydée Oliva,[2] Gregorio Meira[1]

[1]*Instituto de Desarrollo Tecnológico para la Industria Química, INTEC, Universidad Nacional del Litoral–CONICET, Güemes 3450–3000 Santa Fe, Argentina*
[2]*Escuela de Ingeniería Química, Universidad del Zulia, Maracaibo, Venezuela*

Received 10 January 2005; accepted 25 May 2005
DOI 10.1002/app.22902
Published online in Wiley InterScience (www.interscience.wiley.com).

ABSTRACT: A mathematical model is presented that simulates the polymerization of styrene in the presence of polybutadiene (PB) for producing high-impact polystyrene (HIPS) *via* the heterogeneous bulk process. The model follows the polymerization in two phases; and calculates in each phase the main reaction variables and the molecular structure of the three polymeric components: free polystyrene (PS), unreacted PB, and graft copolymer. Two polymerizations (at 90 and 120°C) were carried out and simulated. The model was validated with measurements of the monomer conversion, the grafting efficiencies, and the average molecular weights. © 2006 Wiley Periodicals, Inc. J Appl Polym Sci 99: 3023–3039, 2006

Key words: polystyrene; modeling; molecular weight distribution; morphology

INTRODUCTION

High-impact polystyrene (HIPS) is a composite material containing rubber particles dispersed in a vitreous polystyrene (PS) matrix. The particle diameters (of around 2 μm) are themselves heterogeneous, and typically exhibit "salami" morphologies with vitreous PS occlusions. The rubber phase contains unreacted polybutadiene (PB), graft copolymer, and possibly crosslinked PB. The morphology is generated during the bulk polymerization process. The molecular structure and particle morphology can be modified to satisfy quality requirements of transparency, melt flow index, impact resistance, yield resistance, tensile strength, *etc*.[1–3]

In the bulk process, styrene (St) is polymerized in the presence of 5–10% in weight of dissolved PB, a chemical initiator, an antioxidant (to prevent the rubber crosslinking), and a chain-transfer agent (to control the PS chain lengths). In addition, a mineral oil and a solvent are generally incorporated to reduce the reaction viscosity. The mineral oil remains in the final product.

The industrial HIPS process involves the following stages: rubber dissolution, prepolymerization, finishing, and devolatilization. In the dissolution stage, the rubber is dissolved in the monomer at a relatively low temperature (~70°C), to minimize thermal polymerization. Then the prepolymerization proceeds between 90 and 120°C under well-stirred conditions, up to around 30% conversion. During this stage, the phase separation and the phase inversion processes take place. Between the phase separation and phase inversion, the continuous phase is rich in rubber, while the dispersed phase is rich in PS. During the phase inversion (occurring between 10 and 20% conversion), the morphology is cocontinuous; and thereafter, the continuous phase is the PS-rich phase. After the phase inversion, the particle morphology remains basically unchanged.

The graft copolymer that is produced at the early stages of the prepolymerization reduces the interfacial tension, promotes the phase inversion, and controls the particle size. The initiator half-life is such that the reagent is mostly consumed during the prepolymerization;[4] and during this stage, the rubber grafting is mainly due to the attack of primary initiator radicals onto the allylic H of butadiene (Bd) repeating units. In the finishing stage, the temperature is increased to about 150°C, the system is gently stirred to avoid destroying the developed morphology, and the final conversion reaches around 75%. During the finishing stage, most of the primary radicals are generated by thermal monomer initiation, and the viscosity greatly

Correspondence to: Gregorio R. Meira (gmeira@ceride.gov.ar).
Contract grant sponsors: CONICET, SeCyT and Universidad Nacional del Litoral (Argentina), and FONACYT and CONDES-LUZ (Venezuela).

© 2006 Wiley Periodicals, Inc.

increases.[5] In the final devolatilization stage, the temperature is increased to about 230°C, and vacuum is applied to eliminate the solvent and residual monomer.

The described process is complex because: (a) the reaction proceeds in two immiscible liquid phases; (b) the mass transfer of reagents and products between the phases depends on the following variables that change along the reaction: temperature, viscosity, stirring rate, molar masses, grafting efficiencies, and interface characteristics. By accumulating at the interface, the graft copolymer stabilizes the liquid-liquid dispersion, and constitutes a physical barrier that makes it difficult the mass transfer across the phases.

Many articles have been published in relation with the synthesis and characterization of HIPS.[6–26] Some of the articles[7,16,24,25] have investigated the effects (on the final properties) of the stirring rate, the temperature, the initiator characteristics, and the modifier concentrations. For example, the rubber particle diameters can be made smaller by increasing either the stirring rate or the grafting efficiency.[7] In spite of the industrial importance of the bulk HIPS process, it is somewhat surprising that, so far, only relatively crude heterogeneous models have been developed. For example, the model by Ludwico and Rosen[27] only considers the St homopolymerization, but not the rubber grafting. Homogeneous models are strictly applicable to dilute solution polymerizations. However, several articles have modeled the bulk HIPS process as if it were homogeneous.[28–36] This simplification has been justified by the fact that the partition between the phases of the monomer and initiator are both close to unity. A limitation of homogeneous models is that they underestimate the polydispersity of the global free PS.[34,35]

By assuming that the mass transfer of monomer and initiator is rapid with respect to the polymerization, the HIPS process can be investigated with the aid of multiphase thermodynamics.[4,27,37–41] In relation with the distribution of chemical species between the phases, some of the works have investigated the PS-PB-St blends.[37–41] White and Patel[38] experimentally determined the ternary phase equilibrium of PS, St, and various rubbers (PB and Bd-St copolymers) of different degrees of branching, molecular weights, and microstructure. For PS-St-PB blends, Kruse[39] determined the interaction parameters and partition coefficient of the monomer at 25°C, for polymer concentrations of up to 40% in weight. A complete separation of the polymeric components was observed, and the interaction parameters resulted unaffected by the molecular weights of PS or PB. This behavior was extrapolated to polymer concentrations greater than 40%, by assuming that the monomer partition is independent of the polymer concentration, the level of grafting, or the level of crosslinking.[39] Ludwico and Rosen[41] studied the ternary PS-PB-St system at 25 and 60°C, neglecting the presence of graft copolymer. The emulated polymerizations were homogeneous at conversions between 2 and 5%, and thereafter, heterogeneous.[41] Regarding the distribution of initiators, Ludwico and Rosen[27] measured the partitions of benzoyl peroxide (BPO) and azobisisobutyronitrile (AIBN) in a St-PS-PB system at 0 and 25°C. BPO was seen to slightly prefer the PS-rich phase, and its distribution coefficient was unaffected by conversion, temperature, or the initiator concentration. García *et al*.[42] measured the distribution coefficients of St and *tert*-butyl peroctoate (TBPO) in a St-PS-PB system, emulating conversions below 20%, and for several PS molecular weights. Like BPO, TBPO also concentrates in the PS-rich phase. The monomer was seen to slightly favor the PB-rich phase, and again, no significant variations with temperature were observed.[27,42]

The phase inversion problem has been investigated in several opportunities.[4,43–45] Fisher and Hellmann[4] suggested that the phase inversion occurs when the PS-rich phase volume equals the PB-rich phase volume. In addition, they investigated the role of the graft copolymer in the development of the particle morphology for systems where the molecular weights of the original PB were similar to those of the generated free PS. They concluded that copolymer molecules containing two or more PS branches place themselves at the external interface of the rubber particles, while copolymer molecules with a single PS branch place themselves at the occlusions interface.[4] Also, the particle occlusions are a mixture of free-PS of relatively low molecular weights and PS branches of single-branched copolymer molecules.[4] Jordhamo *et al*.[44] developed a semiempirical expression for predicting the phase inversion of pure PS-PB blends (*i.e.*, not containing low molar mass material). The expression takes into account not only the phase volumes, but also the phase viscosities.[44]

The HIPS mechanical properties are affected by the molecular structure and particle morphology, but their interrelationships are little understood. The global macromolecular structure of HIPS is described by: (a) the MWDs of the free PS, the unreacted PB, and the graft copolymer; and (b) the chemical composition distribution and branching frequency distribution of the graft copolymer. To determine these molecular characteristics, it is first necessary to isolate the three polymeric components by solvent extraction.[6] This procedure is erroneous after the phase inversion, particularly if the rubber particles contain insoluble gels. Even in the absence of gels, it is difficult to quantitatively extract all of the free PS contained in the particle occlusions.[33]

In this work, a mathematical model of a heterogeneous HIPS process is presented. The model was adjusted with *ad hoc* measurements of two almost-iso-

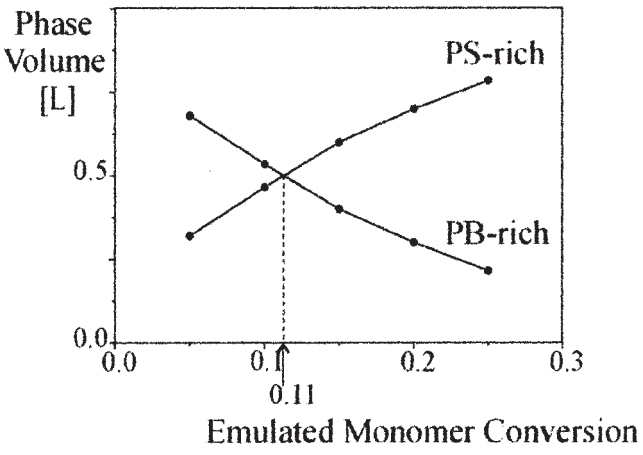

Figure 1 Experimental determination of the equal volume condition, from PB-St-PS mixtures that emulate 5 monomer conversions.

thermal polymerizations; and it predicts the evolution of the phase volumes, the grafting efficiencies, the global concentrations of reagents and products, and the average molecular weights.

EXPERIMENTAL

Phase volumes of PB-St-PS mixtures

Experiments involving PB-St-PS blends were carried out, with the aim of estimating the phase volumes near to the phase inversion. Graft copolymer was not included in the blends, to facilitate the phase separation into two bulk volumes. The experiments were carried out at room temperature to avoid the thermal monomer initiation. Adopting an initial PB load of 6% in weight, five PB-St-PS mixtures were prepared, which emulated monomer conversions of 5, 10, 15, 20, and 25%. The PS molecular weights were $\overline{M}_{w,PS}$ = 171,500 and $\overline{M}_{n,PS}$ = 67,960. The rubber was a medium-*cis*-1,4 PB (Intene Enichem, Italy) of molecular weights: $\overline{M}_{n,PB}$ = 141,000 and $\overline{M}_{w,PB}$ = 283,000. First, the PB-St-PS blends were stirred for 12 h to promote equilibrium. Then, the phase volumes were measured after a neat interface was observed. To this effect, the mixtures were centrifuged at 6000 rpm for periods that varied between 2 and 4 h.

Figure 1 presents the evolution of the phase volumes *versus* the emulated St conversions. The equal volume condition results at a monomer "conversion" of ~11%.

Polymerization reactions

Two (mainly-isothermal) batch polymerizations of St in the presence of 5.14% in weight of PB were carried out. The PB was taken from the same stock as that employed in the PB-St-PS blend experiments, and its initial MWD was measured by size exclusion chromatography (SEC). The St monomer (technical grade by Petrobras Energía S.A., Pto. San Martín, Argentina) was vacuum-distilled. The chemical initiator was BPO (Riedel-de Haën, analytical grade, purity >98%). The solvent was toluene (E. M. Science, Darmstadt, Germany).

The recipes and experimental conditions are given in Table I. Except for the reaction temperature, the two experiments were almost identical. The initial concentrations of monomer, Bd repetitive units, and initiator were: $[St]^0 \cong 7.46$, $[B^*]^0 \cong 0.86$, and $[I_2]^0 \cong 0.0027$ mol/L, respectively. The prepolymerizations were carried out in a 2-L stainless-steel reactor, while the finishing stages were carried out in glass tubes.

The prepolymerization reactor contained an external heating jacket for the isothermal oil, an internal cooling coil for cold water, and a single turbine-type stirrer. Along the prepolymerizations, samples were taken by means of a special sampling device fit at the reactor bottom. The prepolymerizations were as follows. First, the PB was dissolved in the monomer at room temperature for 12 h in a glass flask. Then, the solvent was added until 1 L was completed, and the solution (containing about 10% in volume of toluene) was loaded into the reactor. Nitrogen was bubbled for 10 min to eliminate the dissolved oxygen, and the temperature was raised from room temperature to 70°C at 1°C/min. Then, the initiator was incorporated, the prepolymerizations were started, and the temperature was further increased at 1°C/min until the final reaction temperature was reached [90°C in Exp. 1, and 120°C in Exp. 2; see Figs. 2(a) and 3(a)]. The temperatures were manually controlled by manipulating the heating bath temperature and the flow rate of the internal cooler. Along the prepolymerizations, several 20-mL samples were taken, and the prepolymerizations were stopped when the monomer conversions reached ~30%. The polymer of each sample was precipitated in 200-mL of methanol containing hydroquinone as inhibitor and dry ice to lower the temperature.

For the finishing stage, the prepolymer was loaded into several 10-mm OD glass tubes by means of a vacuum pump. Then, the tubes were sealed and main-

TABLE I
Recipes and Experimental Conditions

	Exp. 1	Exp. 2
St (g)	777.27 (85.695%)	776.58 (85.675%)
Toluene	82.55 (9.10%)	82.64 (9.12%)
Initiator (BPO)	0.5886 (0.065%)	0.5890 (0.065%)
PB	46.62 (5.14%)	46.62 (5.14%)
Temperature (°C)	90[a]	120[a]
Stirring rate (rpm)	125	125

[a] With an initial heating period during the prepolymerization at 1°C/min, starting from 70°C.

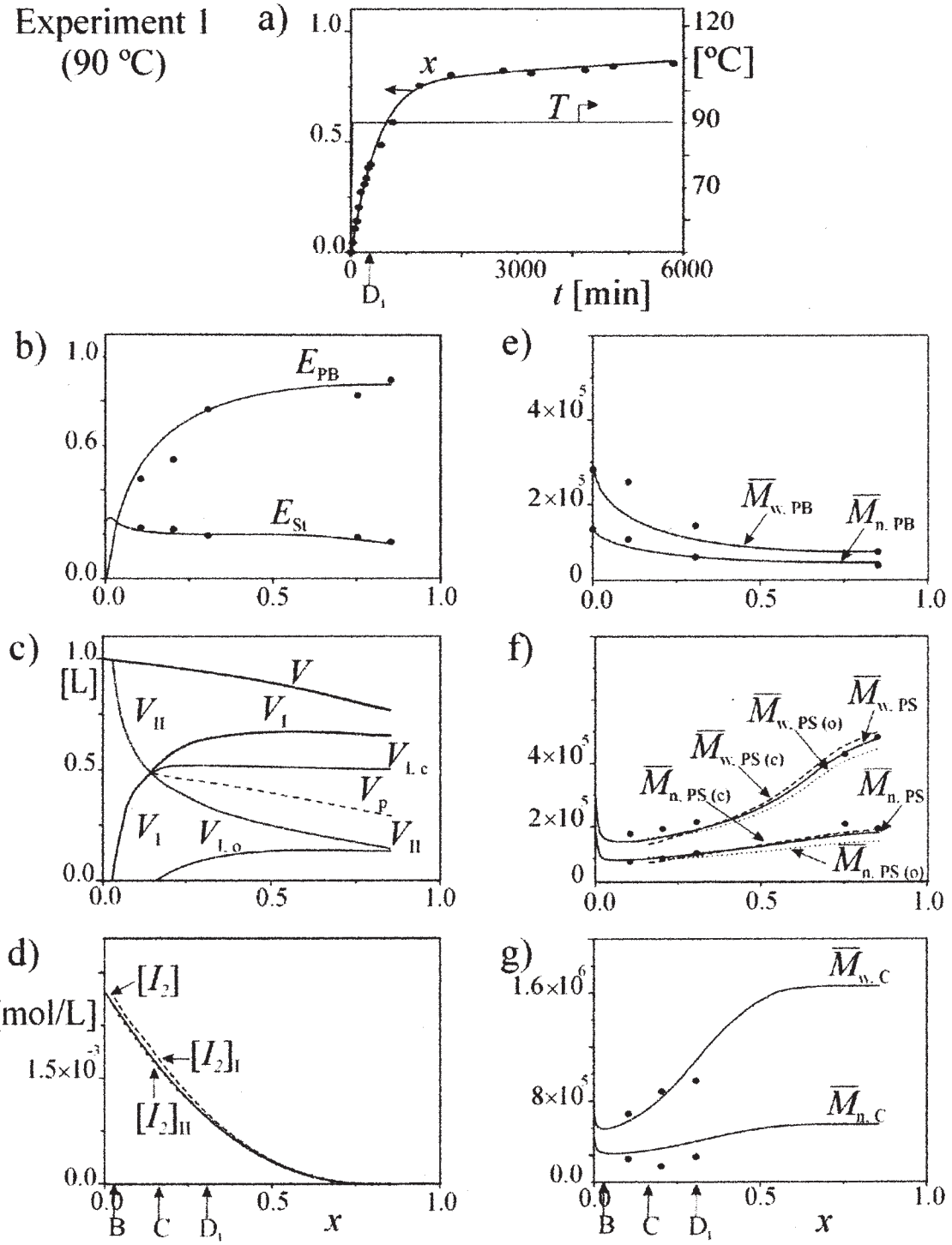

Figure 2 Experiment I with final temperature 90°C: measured and predicted variables. Points B and C represent the predicted phase separation and phase inversion points. D_1 represents the experimental prepolymerization end. (a) Time evolution of temperature and conversion. (b) St and PB grafting efficiencies *versus* conversion. (c) After B, the total predicted volume (V) subdivides into the PS-rich phase volume (V_I) and the PB-rich phase volume (V_{II}). After the phase inversion, V_I subdivides into a continuous phase region, $V_{I,c}$, and an occlusions region $V_{I,o}$; and the total particle volume is $V_P = V_{II} + V_{I,o}$. (d) Predicted evolution of the initiator concentration. (e) Molecular weights of the residual PB. (f) Molecular weights of the free PS. Continuous trace: global free-PS. Dashed trace: PS in continuous phase. Dotted trace: PS in the occlusions region. (g) Molecular weights of the graft copolymer.

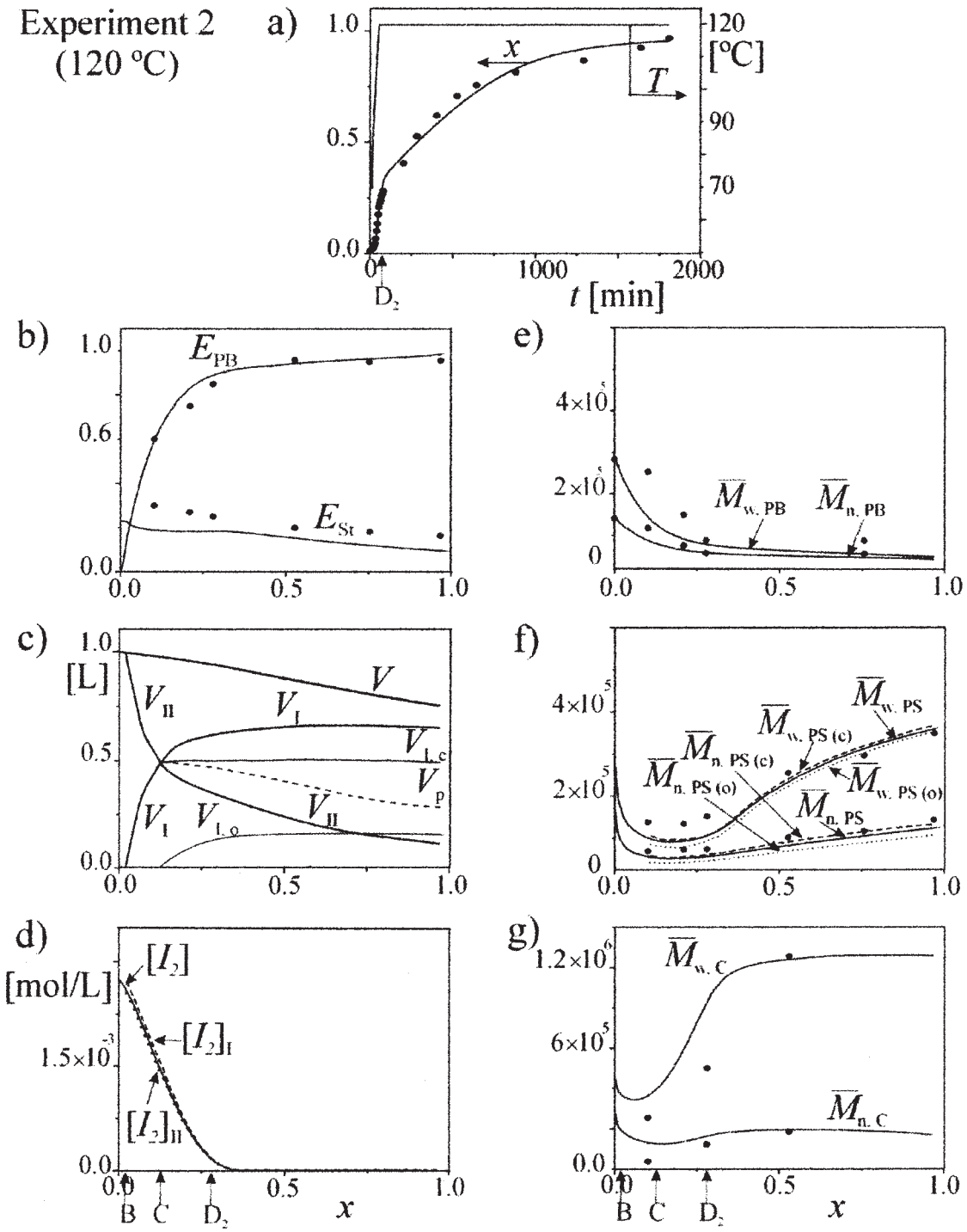

Figure 3 Experiment 2 with final temperature 120°C: measured and predicted variables. Points B and C represent the predicted phase separation and phase inversion points. D_2 represents the experimental prepolymerization end. (a) Time evolution of temperature and conversion. (b) St and PB grafting efficiencies *versus* conversion. (c) After B, the total predicted volume (V) subdivides into the PS-rich phase volume (V_I) and the PB-rich phase volume (V_{II}). After the phase inversion, V_I subdivides into a continuous phase region, $V_{I,c}$, and an occlusions region $V_{I,O}$; and the total particle volume is $V_P = V_{II} + V_{I,O}$. (d) Predicted evolution of the initiator concentration. (e) Molecular weights of the residual PB. (f) Molecular weights of the free PS. Continuous trace: global free-PS. Dashed trace: PS in continuous phase. Dotted trace: PS in the occlusions region. (g) Molecular weights of the graft copolymer.

tained in isothermal baths for 97 h in Exp. 1, and for 29 h in Exp. 2. Along this final stage, the tubes were sampled, introduced into an isopropyllic alcohol–liquid air mixture, broken, and their contents analyzed.

Measurements

The St grafting efficiency strongly determines the particle morphology, and is defined as the mass of grafted St divided by the total mass of polymerized St.[7] The monomer conversion and the St grafting efficiency were determined by solvent-extraction-gravimetry.[33] First, the solvent and the unreacted St were eliminated under vacuum at room temperature until constant weight, and the total polymer mass was measured. Then, the St conversion was calculated by subtraction of the original PB mass. The free PS was extracted from ~0.3 g of the total dry polymer, as follows: (a) 10 mL of methyl ethyl ketone (MEK) were added to the polymer; (b) the mixture was agitated for 12 h in a centrifuge tube, and the tube was centrifuged for 2 h at 7000 rpm; (c) the soluble portion was separated by decantation; (d) ten more milliliters of MEK were added into the insoluble portion, and the procedure was repeated; (e) the two PS solutions were mixed together, the total PS was precipitated with methanol, and the precipitate was dried until constant weight; (f) the centrifuge tube was dried under vacuum until constant weight, and the total mass of insoluble (*i.e.*, the graft copolymer + the unreacted PB) was determined; (g) the grafted PS mass was obtained from the difference between the insoluble mass and initial PB mass; and (h) the St grafting efficiency was obtained from the ratio between the grafted and total bound St masses.

The PB grafting efficiency is the mass of grafted PB (not including the grafted PS) divided by the initial PB mass. The unreacted PB mass, the total copolymer mass, and the PB grafting efficiency were determined through a second solvent extraction procedure applied to the precipitate of graft copolymer and unreacted PB. Petroleum ether was used to dissolve the unreacted PB, but not the graft copolymer. First, 10 mL of petroleum ether with hydroquinone as inhibitor (0.035 g in 50 mL) were added to the precipitate. The system was agitated and centrifuged. The soluble portion was isolated from the graft copolymer, and the procedure was repeated twice. The PB solutions were mixed together, and the unreacted PB was isolated by precipitation in methanol and dried under vacuum. The mass of grafted PB was determined from the difference between the initial PB mass and the unreacted PB mass.

The MWDs and average molecular weights of the isolated polymeric components were determined by SEC. The chromatograph was a Waters 1515 fit with a complete set of 6 μm-Styragel™ columns and a Viscotek 200 detector (containing a specific viscosity sensor and a differential refractometer). The carrier solvent was tetrahydrofuran at 1.0 mL/min, and the system was at ambient temperature. The injection volumes were 0.25 mL at a nominal concentration of 1.0 mg/mL. A "universal" calibration was obtained from a set of PS standards, resulting $\log\{[\eta]M\} = 18.82804 - 0.33507\,V$; where V is the elution volume. The instantaneous intrinsic viscosity $[\eta]$ was obtained from the signals ratio between the specific viscosity and the instantaneous mass, and the molar masses were obtained from the intrinsic viscosity and the universal calibration. At conversions above 60%, the isolated graft copolymer could not be redissolved, and for this reason, their molecular weights could not be determined.

Polymerization results

The experimental results are represented by symbols in Figures 2(a), 2(b), 2(e–g) and 3(a), 3(b), 3(e–g). In Exp. 1, the prepolymerization was stopped at $x = 31\%$, $t = 245$ min [point D_1 in Figs. 2(a), 2(b), 2(e–g)], and in Exp. 2 at $x = 28\%$, $t = 80$ min [point D_2 in Figs. 3(a), 3(b), 3(e–g)]. Polymer characteristics at the end of the prepolymerizations are given in Table II.

The conversions and grafting efficiencies are presented in Figs. 2(a)–3(a) and 2(b)–3(b), respectively. In spite of the shorter reaction time of Exp. 2, its higher temperature produced a final conversion of 97% against 85% in Exp. 1. The PB grafting efficiencies indicate that most of the initial PB was finally grafted.

The average molecular weights of the unreacted PB, free PS, and graft copolymer are represented in Figures 2(e)–2(g) and 3(e)–3(g). As expected, the molecular weights of the residual PB fall monotonically along the reaction, due to the higher probability of grafting of longer chains with respect to shorter chains. In Exp. 2, the molecular weights of the free PS and the graft copolymer are lower than in Exp. 1, as a consequence of the increased chain transfers (to the monomer and to the rubber) at the higher temperature. The average molecular weights of the free PS were measured at conversions >10%, and were seen to continuously grow, due to the steady initiator consumption and to the increasing gel effect. For conversions >10%, the graft copolymer molecular weights grow continuously, because of the grafting-over-grafting process.

Mathematical model

Consider the kinetic mechanism shown in Table III. Like in our previous publication,[33] it assumes the following: chemical and thermal initiation, propagation, transfer to the rubber and to the monomer, termination by recombination, and crosslinking between primary Bd radicals. The nomenclature is as follows: I_2 is the chemical initiator; $I^{\cdot}$ is a primary initiator radical;

TABLE II
Prepolymerization Ends of Experiments 1 and 2

	Exp. 1 (at 245 min)			Exp. 2 (at 80 min)		
	Meas.	Heterog. Model	Homog. Model	Meas.	Heterog. Model	Homog. Model
Conversion	0.31	0.31	0.31	0.28	0.31	0.31
St Grafting Eff.	0.19	0.20	0.20	0.25	0.18	0.16
PB Grafting Eff.	0.76	0.76	0.74	0.85	0.91	0.88
PB: $\overline{M}_{n,\mathrm{PB}}$ [g/mol]	75,000	75,500	80,000	55,000	56,000	57,000
$\overline{M}_{w,\mathrm{PB}}/\overline{M}_{n,\mathrm{PB}}$	1.99	1.55	1.43	1.58	1.32	1.29
PS: $\overline{M}_{n,\mathrm{PS}}$ [g/mol]	117,000	114,000	114,500	75,000	60,000	62,100
$\overline{M}_{w,\mathrm{PS}}/\overline{M}_{n,\mathrm{PS}}$	1.84	1.67	1.51	2.07	2.00	1.92
Cop.: $\overline{M}_{n,\mathrm{C}}$ [g/mol]	385,000	499,000	480,000	322,000	376,000	290,000
$\overline{M}_{w,\mathrm{C}}/\overline{M}_{n,\mathrm{C}}$	2.47	2.20	1.94	2.17	2.98	2.21

S_n is a PS molecule of chain length n; $S^{\cdot}_n$ is a PS homoradical of chain length n; P is a PB or copolymer molecule; $P^{\cdot}_0$ is a primary rubber radical generated on graft copolymer or on unreacted PB; $P^{\cdot}_n$ is a nonprimary copolymer radical with a growing branch containing n repetitive units of St; $P(s,b)$ is a copolymer or an unreacted PB molecule with s repetitive units of St (for the PB homopolymer, it is $s = 0$); [$P^{\cdot}_0(s,b)$ is a primary rubber radical generated by attack to an unreacted Bd unit of $P(s,b)$; $P^{\cdot}_n(s,b)$ is a polystyril radical produced from $P^{\cdot}_0(s,b)$; k_d is the initiator decomposition rate constant; k_{i0} is the rate constant of thermal monomer initiation; k_{i1} k_{i2} k_{i3} are the initiation rate constants; k_p is the propagation rate constant; k_{fm}, k'_{fm} are the constants of chain transfer to the monomer; k_{fg} is the rate constant of transfer to the rubber; and k_{tc}, k'_{tc}, k''_{tc} are the rate constants of recombination termination. In the given mechanism, the following has been neglected: (a) propagation of free radicals with the Bd unit double bonds to produce tetrafunctional branching points and PB-PS crosslinks; (b) intramolecular termination and termination by disproportionation; (c) the (high-temperature) mechanisms of oxidation and polymer degradation; and (d) free-radical intramolecular transfer or backbiting. In addition, the following simplifications are adopted: (a) the reactivity of $S^{\cdot}_1$ radicals coincides with that of any generic $S^{\cdot}_n$; (b) propagation, chain transfer, and recombination termination was unaffected by chain length; and (c) all Bd units exhibit the same (average) reactivity.

Except for the initial homogeneous period that ends at the phase separation, the model calculates the reaction volumes and molecular structures in two phases. The following additional assumptions are adopted: (i) in each phase, the reaction mixture is perfectly stirred; (ii) the initiator is distributed between the phases according with a variable partition coefficient that was determined from data by Ludwico and Rosen,[27] and such coefficient is unaffected by the temperature or molar masses; (iii) the St monomer, the PS chains, and the PB chains are partitioned among the phases according to the ternary diagram of Figure 4 (taken from Ref. 39); (iv) the equilibrium of Figure 4 is unaffected by the temperature, the (PS or PB) molecular weights, or the presence of graft copolymer and solvent; (v) the phase volumes are obtained by simple addition of the chemical species volumes, and the total volume is obtained by addition of the phase volumes; (vi) in each phase, the "gel effect" is a function of the polymer volume fraction;[46] (vii) the phase inversion occurs when the PS-rich phase volume equals the PB-rich phase volume;[4] (viii) after the phase inversion, and due to the increased viscosity, the mass transfer of polymer between the phases stops, and all of the free PS produced in the rubber phase instantaneously accumulates in the particle occlusions; and (ix) the thermal polymerization that may take place during the initial dissolution period is negligible.

The mathematical model is derived in Appendix. Apart from the recipes and reaction conditions, the model requires to input the MWD of the initial PB (not shown). Shortly after the phase separation, the diagram of Figure 4 determines that all the PS chains (both free and grafted) remain in the PS-rich phase (indicated by the subscript I), while all the PB chains (both free and grafted) remain in the PB-rich phase (indicated by the subscript II). The following is calculated in each phase: the volume, the concentration of reagents and products, and the average molecular weights of the free PS, the residual PB, and the graft copolymer. The average molecular weights are obtained from the corresponding weight chain length distributions.

During the initial homogeneous period, a single PB-rich phase (II) exists, and the model eqs. are: (A.1)–(A.16), (A.31)–(A.38), (A.41), (A.47), (A.49), and (A.54). Between the phase separation and phase inversion, eqs. (A.1)–(A.27), (A.31)–(A.38), (A.41), (A.42), (A.47), (A.49), and (A.54) must be solved. After the phase inversion, the model equations are (A.1)–(A.18),

TABLE III
Kinetic Mechanism

Global Kinetics ($n, m = 1, 2, 3,\ldots$)	Detailed Kinetics ($s, s_1, s_2 = 0, 1, 2,\ldots$); ($b, b_1, n, m = 1, 2, 3,\ldots$)
Chemical Initiation	
$I_2 \xrightarrow{k_d} 2\,I^{\cdot}$	$I_2 \xrightarrow{k_d} 2\,I^{\cdot}$
$I^{\cdot} + St \xrightarrow{k_{i1}} S_1^{\cdot}$	$I^{\cdot} + St \xrightarrow{k_{i1}} S_1^{\cdot}$
$I^{\cdot} + P \xrightarrow{k_{i2}} P_0^{\cdot}$	$I^{\cdot} + P(s, b) \xrightarrow{k_{i2}} P_0(s, b)$
Thermal Initiation	
$3\,St \xrightarrow{k_{i0}} 2\,S_1^{\cdot}$	$3\,St \xrightarrow{k_{i0}} 2\,S_1^{\cdot}$
Propagation	
$S_n^{\cdot} + St \xrightarrow{k_p} S_{n+1}^{\cdot}$	$S_n^{\cdot} + St \xrightarrow{k_p} S_{n+1}^{\cdot}$
$P_0^{\cdot} + St \xrightarrow{k_{i3}} P_1^{\cdot}$	$P_0^{\cdot}(s, b) + St \xrightarrow{k_{i3}} P_1^{\cdot}(s, b)$
$P_n^{\cdot} + St \xrightarrow{k_p} P_{n+1}^{\cdot}$	$P_n^{\cdot}(s, b) + St \xrightarrow{k_p} P_{n+1}^{\cdot}(s, b)$
Transfer to the Monomer	
$S_n^{\cdot} + St \xrightarrow{k_{fm}} S_n^{\cdot} + S_1^{\cdot}$	$S_n^{\cdot} + St \xrightarrow{k_{fm}} S_n^{\cdot} + S_1^{\cdot}$
$P_n^{\cdot} + St \xrightarrow{k_{fm}} P + S_1^{\cdot}$	$P_n^{\cdot}(s - n, b) + St \xrightarrow{k_{fm}} P(s, b) + S_1^{\cdot}$
$P_0^{\cdot} + St \xrightarrow{k'_{fm}} P + S_1^{\cdot}$	$P_0^{\cdot}(s, b) + St \xrightarrow{k'_{fm}} P(s, b) + S_1^{\cdot}$
Transfer to the PB or the Copolymer	
$S_n^{\cdot} + P \xrightarrow{k_{fg}} S_n + P_0^{\cdot}$	$S_n^{\cdot} + P(s, b) \xrightarrow{k_{fg}} S_n + P_0^{\cdot}(s, b)$
$P_n^{\cdot} + P \xrightarrow{k_{fg}} P + P_0^{\cdot}$	$P_n^{\cdot}(s - n, b) + P(s_1, b_1) \xrightarrow{k_{fg}} P(s, b) + P_0^{\cdot}(s_1, b_1)$
Termination by Recombination	
$S_n^{\cdot} + S_m^{\cdot} \xrightarrow{k_{tc}} S_{n+m}$	$S_n^{\cdot} + S_m^{\cdot} \xrightarrow{k_{tc}} S_{n+m}$
$P_n^{\cdot} + S_n^{\cdot} \xrightarrow{k_{tc}} P$	$P_{m-n}^{\cdot}(s - m, b) + S_n^{\cdot} \xrightarrow{k_{tc}} P(s, b)$
$P_m^{\cdot} + P_n^{\cdot} \xrightarrow{k_{tc}} P$	$P_{m-n}^{\cdot}(s - s_1 - m, b - b_1) + P_n^{\cdot}(s_1, b_1) \xrightarrow{k_{tc}} P(s, b)$
$P_0^{\cdot} + P_n^{\cdot} \xrightarrow{k''_{tc}} P$	$P_0^{\cdot}(s - s_1 - n, b - b_1) + P_n^{\cdot}(s_1, b_1) \xrightarrow{k''_{tc}} P(s, b)$
$P_0^{\cdot} + S_n^{\cdot} \xrightarrow{k''_{tc}} P$	$P_0^{\cdot}(s - n, b) + S_n^{\cdot} \xrightarrow{k''_{tc}} P(s, b)$
$P_0^{\cdot} + P_0^{\cdot} \xrightarrow{k'_{tc}} P$	$P_0^{\cdot}(s - s_1, b - b_1) + P_0^{\cdot}(s_1, b_1)\, P_{m-n}^{\cdot} \xrightarrow{k'_{tc}} P(s, b)$

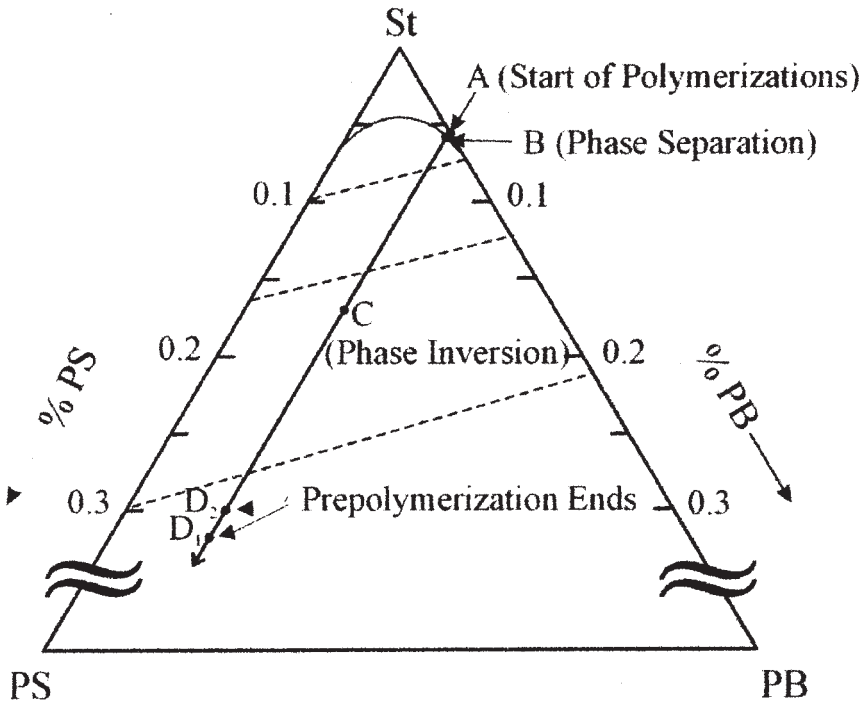

Figure 4 Phase diagram of the St-PB-PS system (adapted from Ref. 39) showing the reaction paths of Experiments 1 and 2.

(A.21)–(A.38), (A.43)–(A.44), (A.47), (A.49), and (A.54). The differential eqs. (A.1)–(A.5) were solved by standard numerical techniques, appropriate for "stiff" differential equations. The differential eqs. (A.41)–(A.44), (A.47), and (A.54) were calculated by direct finite differences, and represent the molecular weight distributions for the free PS (total and in each PS-rich region), the residual PB, and the graft copolymer. The computer program was written in FORTRAN 95 for a Pentium III PC. For each simulated experiment, the computation time was around 2 h.

Table IV presents the adopted model parameters. The initiator efficiency (f), and the Arrhenius expressions for k_{i0}, k_{i1}, k_{i2}, k_{i3}, k_d, k_p, k'_{tc}, and k''_{tc} were directly taken from the literature. The transfer constants were adjusted within published ranges as follows: (a) the transfer to the monomer (k_{fm}) was adjusted to fit the free PS molecular weights; and (b) the transfer to the

TABLE IV
Model Parameters

f		0.5	González *et al.* (1996)[47]
k_d	$[s^{-1}]$	$9.1\times10^{13}\, e^{-29{,}508/RT}$	González *et al.* (1996)[47]
$k_{tc} = k'_{tc} = k''_{tc}$	$\left[\frac{L}{mol\, s}\right]$	$1.7 \times 10^{9}\, e^{-(1667.3/RT) - 2(C_1\psi_i + C_2\psi_i^2 + C_3\psi_i^3)}$(*)	Friis and Hamielec (1976)[46]
$k_P = k_{i1} = k_{i3}$	$\left[\frac{L}{mol\, s}\right]$	$1.0 \times 10^{7}\, e^{-7067/RT}$	Villalobos *et al.* (1991)[48]
k_{i0}	$\left[\frac{L^2}{mol^2\, s}\right]$	$1.1 \times 10^{5}\, e^{-27{,}340/RT}$	Peng (1990)[6]; Yoon and Choi (1995)[49]
$k_{fm} = k'_{fm}$	$\left[\frac{L}{mol\, s}\right]$	$4.414 \times 10^{14}\, e^{-13{,}532/T}$	Adjusted in this work.
k_{i2}	$\left[\frac{L}{mol\, s}\right]$	$2.0 \times 10^{6}\, e^{-7067/RT}$	Estenoz *et al.* (1996a)[33]
k_{fg}	$\left[\frac{L}{mol\, s}\right]$	$1.0487 \times 10^{11}\, e^{-9424.2/T}$	Adjusted in this work.
$K_{I_2}^{-1}$	–	$0.948 + 2.76 \times 10^{-3}\, x$	Adjusted in this work from data by Ludwico *et al.* (1975).[27]

(*) $C_1 = 2.57 - 0.00505\, T$; $C_2 = 9.56 - 0.0176\, T$; $C_3 = -3.03 + 0.00785\, T$; ψ_1 = polymer volume fraction in phase i.

rubber (k_{fg}) was adjusted to fit the St grafting efficiency. We defined the initiator partition coefficient (K_{I2}) as the ratio between the initiator concentration in the PS-rich phase with respect to that in the PB-rich phase [eq. (A.17)]. A linear relationship was adjusted between the inverse of the partition coefficient and conversion (last row of Table IV). K_{I_2} is only slightly larger than 1, thus indicating that the initiator preferentially accumulates in the PS-rich phase. Also, it exhibits a maximum of 1.05 at the beginning of the reaction.

The phase diagram shown in Figure 4 was used to calculate the monomer partition (at all times) and the PS and PB partitions (for a very short period between the phase separation and the condition of total polymer incompatibility). The reaction path is represented by a straight line parallel to the PS-St axis. The solid curve represents the binodal line, above which the system is homogeneous, and the broken lines denote the "tie-lines." Point A represents the start of the polymerizations. The phase separations occur in point B, at a conversion of about 2%. The phase inversions (point C) were calculated with the equal phase volume condition, and according to the model, they occur at $x \cong 13\%$ for both reactions. Points D_1 and D_2 represent the prepolymerization ends of experiments 1 and 2, respectively. From the phase diagram shown in Figure 4, a partition coefficient was calculated for the monomer that is defined as the ratio between the monomer mass fractions in the PS-rich and PB-rich phases [eq. (A.18)]. This coefficient varies with conversion and is lower than 1, thus indicating that the monomer preferentially accumulates in the rubber phase. It attains a maximum value of 0.674 at 97% conversion.

SIMULATION RESULTS AND DISCUSSION

The model predictions are presented in Figures 2 and 3, and in Table II. In general, a quite reasonable agreement with the measurements is observed. The predicted initiator concentrations are shown in Figures 2(d) and 3(d). After the phase separation, the initiator is partitioned between the two phases. The initiator is almost totally consumed at 55% conversion in Exp. 1, and at 25% conversion in Exp. 2.

Figures 2(e) and 3(e) show that $\overline{M}_{w,\mathrm{PB}}$ drops faster than $\overline{M}_{n,\mathrm{PB}}$, due to the higher probability of the larger PB chains to induce grafting. For the free-PS molecular weights, the predictions of Figures 2(f) and 3(f) show an initial drop that was not observed in the measurements. The reason for the high initial PS molecular weights is the (lower) reaction temperatures of the prepolymerization heating ramps. (At lower temperatures, termination by recombination prevails over termination by chain transfer to the monomer.) Between the phase separation and the phase inversion, the free PS is produced in both phases, but it only accumulates in the PS-rich phase. [Even though not shown in Figure 2(f) and due to an increased gel effect, the PS molecular weights produced in the PB-rich phase between the phase inversion and the phase separation are higher than those produced in the PS-rich phase.] After the phase inversion, the free PS accumulates in two regions: the continuous phase [indicated by the subscript (c)], and the particle occlusions [indicated by the subscript (o)]. According to the model, the molecular weights of the free PS contained in the particle occlusions are lower than those of the continuous region; and this result is in accord with observations by Fisher and Hellmann.[4] In the SEC measurements, only the average molecular weights of the global free PS were determined, and their corresponding theoretical predictions are represented by $\overline{M}_{w,\mathrm{PS}}$ and $\overline{M}_{n,\mathrm{PS}}$ in Figures 2(f) and 3(f). Finally, the simulations predict a minimum in the copolymer molecular weights. The initial drop in the copolymer molecular weights is due to the higher probability of grafting of the longer PB chains; the later increase is because of the grafting-over-grafting process [Figs. 2(g) and 3(g)].

Figures 2(c) and 3(c) show the phase volume predictions. The total volume (V) falls along the reaction, due to the system contraction. According to the model, the equal volume condition occurs at ~13% conversion in both experiments, and this value is close to the indirect estimation at room temperature, presented in Figure 1 (11%). However, this verification is not enough evidence of the phase inversion, and additional (morphology and/or viscosity) measurements would be required.[7] After the phase separation, the rubber phase volume steadily decreases while the PS-rich phase increases as a consequence of the migration of PS chains from the PB-rich phase into the PS-rich phases. However, the particle volume (V_{P}) steadily increases due to the occlusions volume. At the reaction ends, the occlusions volume is about 50% of the particles volume in Exp. 1, and about 40% of the particles volume in Exp. 2.

Finally, a comparison with an equivalent homogeneous model was carried out. The homogeneous model predictions were also produced by the heterogeneous model, by simply setting to 1 all of the partition coefficients (of the initiator, the monomer, the PS chains, and the PB chains). Table II presents the homogeneous model results for the global polymer characteristics at the end of the prepolymerizations. As expected, the homogeneous model predicts lower polydispersities for the free PS. In the final product, these differences are further increased, and for example in Exp. 2, the free-PS polydispersity is 2.70 according to the homogeneous model, and 2.91 according to the heterogeneous model.

CONCLUSIONS

An heterogeneous model has been presented that calculates the detailed molecular structure and phase volumes along a batch HIPS process. Even though the model cannot predict the particle and occlusion diameters, this is a first step toward such objective, which will be the subject of a future communication. All of the measurements were in reasonable accord with the theoretical predictions, and only minor adjustments were needed in two chain transfer constants. Some of the theoretical predictions could not be experimentally verified, but they are (at least qualitatively) in agreement with previous publications. An example of this is the lower molecular weights of the final occluded PS with respect to the molecular weights of PS in the continuous phase. For this reason, the polydispersity of the final global free-PS is larger than that of an equivalent homogeneous polymerization.[34,35]

The phase inversion was assumed to occur at the condition of equal phase volumes. The exact determination of the phase inversion is experimentally and theoretically complex. However, a good prediction of the phase inversion seems crucial for an adequate estimation of the particle morphology. Another important model assumption was that (after the phase inversion) the occlusions volume is initially zero. This could be relaxed by assuming that the initial occlusions volume is made up of PS branches belonging to single-branched copolymer molecules.[4]

The melt flow index is an important process-control variable, that is a measure of the melt viscosity after devolatilization. The present model could be extended for predicting the melt flow index of the final product on the basis of the PS molecular weights, the phase volumes, and the mineral oil content (if this compound is incorporated in the material).[50]

NOMENCLATURE

b	total repetitive units of Bd, dimensionless
Bd	butadiene
B^*	unreacted Bd unit
C	graft copolymer
E_{St}	St grafting efficiency, dimensionless
E_{PB}	PB grafting efficiency, dimensionless
f	initiator efficiency, dimensionless
G	mass, g
G_i	mass of i, i = GS, PS, PB, T, g
$G_{PS}(n)$	WCLD of free PS, g
$G_C(s,b)$	WCLD of copolymer, g
$G_{PB}(b)$	WCLD of residual PB, g
GS	mass of grafted PS, g
$I^{\cdot}$	primary initiator radical
I_2	chemical initiator
k_d	initiator decomposition rate constant, s^{-1}
k_{fg}	rate constant of chain transfer to the rubber, L/mol s^{-1}
k_{fm},k'_{fm}	rate constants of chain transfer to the monomer, L/mol s^{-1}
k_{i0}	rate constant of thermal monomer initiation, L^2/mol^2 s^{-1}
k_{i1},k_{i2},k_{i3}	initiation rate constants, L/mol s^{-1}
k_p	propagation rate constant, L/mol s^{-1}
k_{tc},k'_{tc},k''_{tc}	rate constants of recombination termination, L/mol s^{-1}
K_{I_2}	initiator partition coefficient
M_{Bd}, M_{St}	molecular weight of Bd and St, g/mol
MWD	molecular weight distribution
N	number of moles
NCLD	number chain-length distribution
P	residual PB or copolymer molecule with (many) ungrafted Bd units
$P(s,b)$	P molecule with s repetitive units of St and b units of Bd. In the case of PB, it is $s = 0$
$P^{\cdot}$	generic Bd radical
$P^{\cdot}_0$	primary rubber radical generated by attack of an unreacted Bd unit contained in P
$P^{\cdot}_0(s,b)$	primary rubber radical, generated from an attacked Bd unit of P(s,b)
$P^{\cdot}_n$	nonprimary copolymer radical with a new growing branch containing n repetitive units of St
$P^{\cdot}_n(s,b)$	radical produced after an attack to P(s,b)
PB	polybutadiene
PS	polystyrene
R_p	global rate of St consumption, mol/L s^{-1}
R_{PPS_i}	generation rate of PS in phase i, i = I, II, mol/L s^{-1}
R_{PGS_i}	generation rate of GS in phase i, i = I, II, mol/L s^{-1}
s	total repetitive units of St, dimensionless
S_n	PS molecule of chain length n
$S^{\cdot}$	St radical
$S^{\cdot}_n$	PS homoradical of chain length n
St	styrene
t	time, s
T	temperature, °C
V	volume, L
WCLD	weight chain-length distribution
x	monomer conversion, dimensionless
[ ]	molar concentration, mol/L

Greek letters

$\alpha,\beta,\varphi,\gamma,\tau,\tau_1$	dimensionless kinetic parameters
ρ_k	density of chemical species k, k = St, PB, PS, T, g/L
θ_i	mass fractions of i, i = PS, St, PB, dimensionless
ψ	polymer volume fraction, dimensionless

Subscripts

c, o continuous phase and the particle occlusions regions
I, II PS-rich and PB-rich phases
p particle
T toluene

Superscripts

0 initial condition

APPENDIX: MATHEMATICAL MODEL

Global mass balances

Let us indicate the PS-rich and PB-rich phases with the subscripts I and II, respectively. For any generic species j, $[j]$ represents its global molar concentration (in mol/L), and N_j the total number of moles. In addition, $[j]_I$ and $[j]_{II}$ are the molar concentrations of j in phase I and II, respectively. Consider the mass balances of reagents and products along a two-phase polymerization.

(a) *Initiator:*

$$\frac{d}{dt} N_{I_2} = -k_d([I_2]_I V_I + [I_2]_{II} V_{II}) \tag{A.1}$$

(b) Monomer:

$$\frac{d}{dt} N_{St} = -k_P\{[St]_I([S^\cdot]_I + [P^\cdot]_I)V_I + [st]_{II}([S^\cdot]_{II} + [P^\cdot]_{II})V_{II}\} = -R_p V \tag{A.2}$$

where R_p is the global polymerization rate (in mol/L s).

(c) Unreacted Bd *Units (B*): B** is any unreacted Bd unit contained either in a copolymer molecule or in an unreacted PB molecule. We can write:

$$\frac{d}{dt} N_{B^*} = -\{k_{i2}[I^\cdot]_I + k_{fg}([P^\cdot]_I + [S^\cdot]_I)\}[B^*]_I V_I + k'_{fm}[St]_I[P_0^\cdot]_I V_I - \{k_{i2}[I^\cdot]_{II} + k_{fg}([P^\cdot]_{II} + [S^\cdot]_{II}V_{II} + k'_{fm}[St]_{II}[P_0^\cdot]_{II}V_{II} \tag{A.3}$$

(d) Total mass of grafted PS *and of free* PS *(G_{GS} and G_{PS}, respectively):*

$$\frac{d}{dt} G_{GS} = \frac{d}{dt}(G_{GS_I} + G_{GS_{II}}) = R_{p_{GS_I}} M_{St} V_I + R_{p_{GS_{II}}} M_{St} V_{II} \tag{A.4}$$

$$\frac{d}{dt} G_{PS} = \frac{d}{dt}(G_{PS_I} + G_{PS_{II}}) = R_{p_{PS_I}} M_{St} V_I + R_{p_{PS_{II}}} M_{St} V_{II} \tag{A.5}$$

where M_{st} (= 104 g/mol) is the monomer molecular weight; $R_{p_{GSi}}$ and $R_{p_{PS_i}}$ (for i = I, II) are the polymerization rates yielding graft and free PS, respectively. These reaction rates are calculated through:

$$R_{p_{PS_i}} = \frac{[S^\cdot]_i}{[S^\cdot]_i + [P^\cdot]_i} R_{Pi} \frac{(k_{fm}[St]_i + k_{fg}[B^*]_i + k_{tc}[S^\cdot]_i)}{(k_{fm}[St]_i + k_{fg}[B^*]_i + k_{tc}([S^\cdot]_i + [P^\cdot]_i) + k''_{tc}[P_0^\cdot]_i)} \quad i = \text{I,II} \tag{A.6}$$

$$R_{p_{GS_i}} = \frac{[P^\cdot]_i}{[S^\cdot]_i + [P^\cdot]_i} R_{Pi} + \frac{[S^\cdot]_i}{[S^\cdot]_i + [P^\cdot]_i} \times R_{Pi} \frac{(k_{tc}[P^\cdot]_i + k''_{tc}[P_0^\cdot]_i)}{(k_{fm}[St]_i + k_{fg}[B^*]_i + k_{tc}([S^\cdot]_i + [P^\cdot]_i) + k''_{tc}[P_0^\cdot]_i)} \quad i = \text{I,II} \tag{A.7}$$

with:

$$R_{Pi} = k_P[St]_i([P^\cdot]_i + [S^\cdot]_i) \quad i = \text{I,II} \tag{A.8}$$

(e) Global free radicals with pseudo-steady-state assumption:

$$\frac{d}{dt}([I^\cdot]_i V_i) = (2fk_d[I_2]_i - k_{i1}[St]_i[I^\cdot]_i - k_{i2}[I^\cdot]_i[B^*]_i)V_i \cong 0 \quad i = \text{I,II} \tag{A.9}$$

$$\frac{d}{dt}\{[S_1^\cdot]_i V_i\} = k_{i1}[I^\cdot]_i[St]_i V_i + 2k_{i0}[st]_i^3 V_i + k_{fm}[St]_i([S^\cdot]_i + [P^\cdot]_i)V_i + k'_{fm}[St]_i[P_0^\cdot]_i V_i - \{k_P[st]_i + k_{fg}[B^*]_i + k_{fm}[St]_i\} \times [S_1^\cdot]_i V_i - \{k''_{tc}[P_0^\cdot]_i + k_{tc}([S^\cdot]_i + [P^\cdot]_i)\}[S_1^\cdot]_i V_i \cong 0 \quad i = \text{I,II} \tag{A.10}$$

$$\frac{d}{dt}\{[S_n^\cdot]_i V_i\} = k_P[St]_i[S_{n-1}^\cdot]_i V_i - \{k_P[st]_i + k_{fm}[St]_i\}[S_n^\cdot]_i V_i - \{k_{fg}[B^*]_i + k''_{tc}[P_0^\cdot]_i + k_{tc}([S^\cdot]_i + [P^\cdot]_i)\}[S_n^\cdot]_i V_i \cong 0 \quad n = 2,3,\ldots i = \text{I,II} \tag{A.11}$$

$$\frac{d}{dt}([P_0^\cdot]_i V_i) = \{(k_{i2}[I^\cdot]_i + k_{fg}([S^\cdot]_i + [P^\cdot]_i))[B^*]_i - (k_{i3}[St]_i + k'_{fm}[St]_i + k'_{tc}[P_0^\cdot]_i + k''_{tc}([S^\cdot]_i + [P^\cdot]_i)) \times [P_0^\cdot]_i\} V_i \cong 0 \quad i = \text{I,II} \tag{A.12}$$

$$\frac{d}{dt} = \{[P_i^{\cdot}]_i V_i\} = k_{i3}[\mathrm{St}]_i[P_0^{\cdot}]_i V_i - (k_p + k_{fm})[\mathrm{St}]_i[P_1^{\cdot}]_i V_i - \{k_{fg}[B^*]_i + k''_{tc}[P_0^{\cdot}]_i + k_{tc}([S^{\cdot}]_i + [P^{\cdot}]_i)\}[P_1^{\cdot}]_i V_i \cong 0 \quad i = \mathrm{I,II} \quad (A.13)$$

$$\frac{d}{dt}\{[P_n^{\cdot}]_i V_i\} = k_P[\mathrm{St}]_i[P_{n-1}^{\cdot}]_i V_i - (k_P + k_{fm})[\mathrm{St}]_i[P_n^{\cdot}]_i V_i - \{k_{fg}[B^*] + k''_{tc}[P_0^{\cdot}]_i + k_{tc}([S^{\cdot}]_i + [P^{\cdot}]_i)\}[P_n^{\cdot}]_i V_i \cong 0 \quad n = 2,3,\ldots i = \mathrm{I,II} \quad (A.14)$$

Adding up eq. (A.10) with eqs. (A.11) over all n's; and eq. (A.13) with eqs. (A.14) over all n's, it results:

$$\frac{d}{dt}([S^{\cdot}]_i V_i) = \{k_{i1}[\mathrm{St}]_i[I^{\cdot}]_i + 2k_{i0}[\mathrm{st}]_i^3 + k'_{fm}[\mathrm{St}]_i[P_0^{\cdot}]_i + k_{fm}[\mathrm{St}]_i[P^{\cdot}]_i - k_{fg}[B^*]_i[S^{\cdot}]_i - k''_{tc}[P_0^{\cdot}]_i[S^{\cdot}]_i - k_{tc}([S^{\cdot}]_i + [P^{\cdot}]_i)[S^{\cdot}]_i\} V_i \cong 0 \quad i = \mathrm{I,II} \quad (A.15)$$

$$\frac{d}{dt}([P^{\cdot}]_i V_i) = k_{i3}[\mathrm{St}]_i[P_0^{\cdot}]_i V_i - \{k_{fm}[\mathrm{St}]_i + k_{fg}[B^*]_i + k_{tc}([S^{\cdot}]_i + [P^{\cdot}]_i) + k''_{tc}[P_0^{\cdot}]_i\}[P^{\cdot}]_i V_i \cong 0 \quad i = \mathrm{I,II} \quad (A.16)$$

Distribution of reagents and products between the phases

The initiator partition coefficient $K_{I_2}(x)$ is defined on the basis of the molar concentrations, as follows:

$$K_{I_2}(x) = \frac{[I_2]_\mathrm{I}}{[\mathrm{I}_2]_\mathrm{II}} \quad (A.17)$$

The inverse of the partition coefficient exhibits a slight linear dependence with conversion (see Table IV). The partition coefficients for the monomer, solvent, PS, and PB, are based on their mass fractions. The partitions of St, PS, and PB are obtained from the phase diagram shown in Figure 4, and are defined as follows:

$$\theta_{St} = \frac{[\mathrm{St}]_I V_I / G_I}{[\mathrm{St}]_{II} V_{II} / G_{II}} \quad (A.18)$$

$$\theta_{PS} = \frac{(G_{\mathrm{PS_I}} + G_{\mathrm{GS_I}})/G_\mathrm{I}}{(G_{\mathrm{PS_{II}}} + G_{\mathrm{GS_{II}}})/G_\mathrm{II}} \quad (A.19)$$

$$\theta_{PB} = \frac{[B^*]_\mathrm{I} V_\mathrm{I} / G_\mathrm{I}}{[B^*]_\mathrm{II} V_\mathrm{II} / G_\mathrm{II}} \quad (A.20)$$

where G_I and G_II are the total masses of phases I and II, respectively.

Neglecting the initiator contribution, the total reaction mass is:

$$G_\mathrm{I} + G_\mathrm{II} = G_\mathrm{PS} + G_\mathrm{PB}^0 + G_\mathrm{GS} + N_\mathrm{St} M_\mathrm{St} + G_\mathrm{T} \quad (A.21)$$

where GT is the total toluene mass. In turn, the phase volumes are:

$$G_\mathrm{I} = [\mathrm{St}]_\mathrm{I} V_\mathrm{I} M_\mathrm{St} + G_{\mathrm{PS_I}} + [B^*]_\mathrm{I} V_\mathrm{I} M_\mathrm{Bd} + G_{\mathrm{GS_I}} + G_\mathrm{T} \times \frac{G_\mathrm{I}}{(G_\mathrm{I} + G_\mathrm{II})} \quad (A.22)$$

$$G_\mathrm{II} = [\mathrm{St}]_\mathrm{II} V_\mathrm{II} M_\mathrm{St} + G_{\mathrm{PS_{II}}} + [B^*]_\mathrm{II} V_\mathrm{II} M_\mathrm{Bd} + G_{\mathrm{GS_{II}}} + G_\mathrm{T} \times \frac{G_\mathrm{II}}{(G_\mathrm{I} + G_\mathrm{II})} \quad (A.23)$$

Equations (A.22) and (A.23) imply that the solvent is equally partitioned among the phases.

The total mass of polymerized St is:

$$(G_\mathrm{PS} + G_\mathrm{GS}) = (G_{\mathrm{PS_I}} + G_{\mathrm{GS_I}}) + (G_{\mathrm{PS_{II}}} + G_{\mathrm{GS_{II}}}) \quad (A.24)$$

Volumes

After the phase separation, the total reaction volume V is:

$$V = V_\mathrm{I} + V_\mathrm{II} \quad (A.25)$$

Assuming volume additivity and a negligible consumption of PB double bonds, due to grafting, the phase volumes are:

$$V_\mathrm{I} = [\mathrm{St}]_\mathrm{I} V_\mathrm{I} M_\mathrm{St}/\rho_\mathrm{St} + [B^*]_\mathrm{I} V_\mathrm{I} M_\mathrm{Bd}/\rho_\mathrm{PB} + (G_{\mathrm{PS_I}} + G_{\mathrm{GS_I}})/\rho_\mathrm{PS} + \left[G_\mathrm{T} \times \frac{G_\mathrm{I}}{(G_\mathrm{I} + G_\mathrm{II})}\right]/\rho_\mathrm{T} \quad (A.26)$$

$$V_\mathrm{II} = [\mathrm{St}]_\mathrm{II} V_\mathrm{II} M_\mathrm{St}/\rho_\mathrm{St} + [B^*]_\mathrm{II} V_\mathrm{II} M_\mathrm{Bd}/\rho_\mathrm{PB} + (G_{\mathrm{PS_{II}}} + G_{\mathrm{GS_{II}}})/\rho_\mathrm{PS} + \left[G_\mathrm{T} \times \frac{G_\mathrm{II}}{(G_\mathrm{I} + G_\mathrm{II})}\right]/\rho_\mathrm{T} \quad (A.27)$$

where ρk is the density of chemical species k.

After the phase inversion, the PS-rich phase is subdivided into two regions: the continuous phase and the particle occlusions (represented by subscripts c and o, respectively). Thus, after the phase inversion, it is:

$$V_\mathrm{I} = V_{\mathrm{I,c}} + V_{\mathrm{I,o}} \quad (A.28)$$

with:

$$V_{I,o} = \frac{G_{PS,o}}{\rho_{PS}\left(1 - \frac{[St]_I M_{St}}{\rho_{St}}\right)} \quad (A.29)$$

and $V_{I,o} = 0$ at the phase inversion. In addition, the particles volume is:

$$V_P = V_{II} + V_{I,o} \quad (A.30)$$

Monomer conversion (x) and styrene grafting efficiency (E_{St})

$$x = \frac{N^0_{St} - N_{St}}{N^0_{St}} \quad (A.31)$$

$$E_{St} = \frac{G_{GS}}{G_{GS} + G_{PS}} \quad (A.32)$$

Weight chain-length distribution (WCLD) of the free PS

Let us first define the following dimensionless parameters:

$$\varphi_i = \frac{[S^\cdot]_i}{[S^\cdot]_i + [P^\cdot]_i} \quad i = I,II \quad (A.33)$$

$$\beta_i = \frac{k_{tc} R_{Pi}}{(k_P[st]_i)^2} \quad i = I,II \quad (A.34)$$

$$\tau_i = \frac{k_{fm}}{k_P} + \frac{k_{fg}[B^*]_i}{(k_P[st]_i)} + \gamma_i \tau_{1i} \; i = I,II \quad (A.35)$$

$$\tau_{1i} = \frac{k''_{tc} R_{Pi}}{(k_P[st]_i)^2} \quad i = I,II \quad (A.36)$$

$$\gamma_i = \frac{[P^\cdot_0]_i}{[S^\cdot]_i + [P^\cdot]_i} \quad i = I,II \quad (A.37)$$

$$\alpha_i = \tau_i + \beta_i \; i = I,II \quad (A.38)$$

From the global mechanism of Table III, the number chain-length distribution (NCLD) of the total free-PS is obtained from:

$$\frac{d}{dt}N_{PS}(n) = \left\{(k_{fm}[St]_I + k_{fg}[B^*]_I)[S^\cdot_n]_I V_I + \frac{k_{tc}}{2}\sum_{m=1}^{n-1}[S^\cdot_m]_I[S^\cdot_{n-m}]_I V_I\right\} + \left\{(k_{fm}[St]_{II} + k_{fg}[B^*]_{II})[S^\cdot_n]_{II} V_{II} + \frac{k_{tc}}{2}\sum_{m=1}^{n-1}[S^\cdot_m]_{II}[S^\cdot_{n-m}]_{II} V_{II}\right\} = \sum_i \left\{(k_{fm}[St]_i + k_{fg}[B^*]_i)[S^\cdot_n]_i V_i + \frac{k_{tc}}{2}\Sigma^{n-1}_{m=1}[S^\cdot_m]_i[S^\cdot_{n-m}]_i V_i\right\}$$
$$n = 1,2,3,\ldots i = I,II \quad (A.39)$$

Considering eqs. (A.8), (A.10), (A.11), (A.15), and (A.33)–(A.38), and operating as in Estenoz et al.[33] the following is obtained:

$$\frac{d}{dt}N_{PS}(n) = \sum_i \left\{[R_{Pi} V_i \varphi_i(\tau_i - \gamma_i \tau_{1i})]\alpha_i^{-\alpha_i n} + \left[\frac{R_{Pi} V_i \varphi_i^2 \beta_i}{2}\right]\alpha_i^2 n e^{-\alpha_i n}\right\}$$
$$n = 1,2,3,\ldots i = I,II \quad (A.40)$$

The right-hand side of eq. (A.40) represents the NCLD of the total instantaneously-produced PS. Such distribution is the sum of the instantaneous distributions that are produced in each phase. Let us multiply each of eqs. (A.40) by the corresponding molecular weights (nMSt), yielding:

$$\frac{d}{dt}G_{PS}(n) = \frac{d}{dt}[G_{PS_I}(n) + G_{PS_{II}}(n)] = \sum_i \left\{\left[R_{Pi} V_i \varphi_i \frac{(\tau_i - \gamma_i \tau_{1i})}{\alpha_i} + \frac{R_{Pi} V_i \varphi_i^2 \beta_i}{2} n\right]\alpha_i^2 M_{Si} n e^{-\alpha}{}_i n\right\}$$
$$n = 1,2,3,\ldots i = I,II \quad (A.41)$$

The cumulative WCLD of the total free-PS is obtained by integration of eq. (A.41). For the very short period immediately following the phase separation, two thermodynamically-compatible phases coexist. Assuming that the partitions are unaffected by the molecular weights, eq. (A.19) can be applied to each individual PS species; and the WCLD in each phase (represented by $G_{PSi}(n)$, i = I,II) can be calculated through eqs. (A.1)–(A.27), (A.33)–(A.38), and (A.41). After the PS and PB chains become incompatible and until the phase inversion, the free PS only accumulates in the PS-rich phase, and $G_{PS_{II}} = 0$. The WCLD of the total PS that accumulates in phase I during the heterogeneous period that finishes at the phase inversion is given by:

$$\frac{d}{dt}G_{PS_I}(n) = \sum_i \left\{\left[R_{Pi} V_i \varphi_i \frac{(\tau_i - \gamma_i \tau_{1i})}{\alpha_i} + \frac{R_{Pi} V_i \varphi_i^2 \beta_i}{2} n\right]\alpha_i^2 M_{Si} n e^{-\alpha_i n}\right\} n = 1,2,3,\ldots$$
$$i = I,II \quad (A.42)$$

During this period, eqs. (A.1)–(A.18), (A.21)–(A.27), (A.33)–(A.38), and (A.42) must be simultaneously solved.

After the phase inversion, we must keep track of the free PS that accumulates in the particle occlusions region and in the continuous phase region, as follows:

$$\frac{d}{dt}G_{PS_{I,o}}(n) = \left[\frac{\tau_1}{\alpha_I} + \frac{\beta_I}{2}n\right]R_{PI}V_{I,o}\alpha_I^2 M_{St}ne^{-\alpha_I n} + \left[\frac{(\tau_{II} - \gamma_{II}\tau_{1_{II}})}{\alpha_{II}} + \frac{\varphi_{II}\beta_{II}}{2}n\right]\varphi_{II}R_{PII}V_{II}\alpha_{II}^2 M_{St}ne^{-\alpha_{II}n} \quad n = 1,2,3.\ldots \quad \text{(A.43)}$$

$$\frac{d}{dt}G_{PS_{I,c}}(n) = \left[\frac{\tau_1}{\alpha_I} + \frac{\beta_I}{2}n\right]R_{PI}V_{I,c}\alpha_I^2 M_{St}ne^{-\alpha_I n} \quad n = 1,2,3,\ldots \quad \text{(A.44)}$$

After the phase inversion, eqs. (A.1)–(A.18), (A.21)–(A.29), (A.33)–(A.38), (A.43)–(A.44) must be simultaneously solved for calculating the WCLDs of the free PS that accumulates in each of the two PS-rich regions: the continuous phase and the particle occlusions.

WCLD of the unreacted PB

Following a similar treatment to that of Estenoz et al.,[33] the NCLD of the unreacted PB, $N_{PB}(b)$, is given by:

$$\frac{d}{dt}N_{PB}(b) = \Sigma_i\left\{-[k_{i2}[I^{\cdot}]_i + k_{fg}([S^{\cdot}]_i + [P^{\cdot}]_i)]bN_{PBi}(b) + k'_{fm}[St]_i[P_0^{\cdot}]_i\frac{bN_{PBi}(b)}{[B^*]_i^{\cdot}}\right\}b = 1,2,3\ldots i = I,II \quad \text{(A.45)}$$

Introducing eqs. (A.3), (A.12), (A.16), and (A.33)–(A.38) into eq. (A.45), it results:

$$\frac{d}{dt}N_{PB}(b) = \Sigma_i\left\{-R_{Pi}V_i(1-\varphi_i)\left(\tau_i - \gamma_i\tau_{1i} + \beta_i\varphi_i + \frac{\gamma_i\tau_{1i}\varphi_i}{1-\varphi_i}\right)\frac{bN_{PBi}(b)}{[B^*]_iV_i} - R_{Pi}V_i(1-\varphi_i)[\beta_i(1-\varphi_i) + 2\gamma_i\tau_{1i}]\frac{bN_{PBi}(b)}{[B^*]_iV_i} - \frac{R_{Pi}^2\gamma_i^2V_ik'_{tc}bN_{PBi}(b)}{(k_P[St]_i)^2\ [B^*]_iV_i}\right\}b = 1,2,3,\ldots i = I,II \quad \text{(A.46)}$$

The WCLD of the residual PB is obtained by multiplying each of eqs. (A.46) by their corresponding molecular weights (bM_{Bd}), resulting:

$$\frac{d}{dt}G_{PB}(b) = \frac{d}{dt}[G_{PB_I}(b) + G_{PB_{II}}(b)] = \Sigma_i\left\{-R_{Pi}V_i(1-\varphi_i)\left(\tau_i - \gamma_i\tau_{1i} + \beta_i\varphi_i + \frac{\gamma_i\tau_{1i}\varphi_i}{1-\varphi_i}\right)\frac{b^2N_{PBi}(b)M_{Bd}}{[B^*]_iV_i} - R_{Pi}V_i(1-\varphi_i)[\beta_i(1-\varphi_i) + 2\gamma_i\tau_{1i}]\frac{b^2N_{PBi}(b)M_{Bd}}{[B^*]_iV_i} - \frac{R_{Pi}^2\gamma_i^2V_ik'_{tc}b^2N_{PBi}(b)M_{Bd}}{(k_P[st]_i)^2\quad [B^*]_iV_i}\right\}b = 1,2,3,\ldots i = I,II \quad \text{(A.47)}$$

with

$$G_{PB} = \Sigma_b G_{PB}(b) \quad b = 1,2,3,\ldots \quad \text{(A.48)}$$

The WCLD of the unreacted PB in each phase is initially calculated through eqs. (A.1)–(A.27), (A.33)–(A.38), and (A.47), together with the assumption that the partition of each PB species is independent of the molecular weight. After the PS and PB chains become totally incompatible, the PB only accumulates in the PB-rich phase (i.e.,$G_{PB_I} = 0$), and eqs. (A.1)–(A.18), (A.21)–(A.27), (A.33)–(A.38), and (A.47) must be simultaneously solved.

The PB grafting efficiency is the mass of reacted PB divided by the initial PB mass G_{PB}^0, i.e.,

$$E_{PB} = \frac{G_{PB}^0 - G_{PB}}{G_{PB}^0} \quad \text{(A.49)}$$

Bivariate weight chain length distribution of the graft copolymer

Let us represent with $B^*(s,b)$ any unreacted Bd unit of $P(s,b)$; where s and b represent the number of St and Bd repetitive units, respectively. The mass balance for the primary rubber radicals results:

$$\frac{d}{dt}\{[P_0^{\cdot}(s,b)]_iV_i\} = \{k_{i2}[I^{\cdot}]_i + k_{fg}([S^{\cdot}]_i + [P^{\cdot}]_i)\}[B^*]_iV_i - \{k_{i3}[St]_i + k'_{fm}[St]_i + k'_{tc}[P_0^{\cdot}]_i + k''_{tc}([S^{\cdot}]_i + [P^{\cdot}]_i)\} \times [P_0^{\cdot}(s,b)]_iV_i \cong 0 \quad s = 0,1,2,\ldots \quad b = 1,2,3,\ldots i = I,II \quad \text{(A.50)}$$

Comparing eqs. (A.12) and (A.50), one finds that:

$$\frac{[P_0^{\cdot}(s,b)]_i}{[P_0^{\cdot}]_i} = \frac{[B^*(s,b)]_i}{[B^*]_i} \quad s = 0,1,2\ldots \quad b = 1,2,3\ldots i = I,II \quad \text{(A.51)}$$

Equation (A.51) suggests that the fraction of primary rubber radicals generated from any $P(s,b)$ species with

respect to the total number of primary rubber radicals coincides with the molar fraction of unreacted B* units in those same species with respect to the total B* units. Thus, the bivariate NCLD for the accumulated copolymer is obtained from:

$$\frac{d}{dt}\{[P(s,b)]V\} = \Sigma_i\{T_{1_i} + T_{2_i} + T_{3_i} + T_{4_i} + T_{5_i}\}$$
$$s,b = 1,2,3,\ldots\ i = \text{I,II} \quad \text{(A.52a)}$$

with:

$$T_{1_i} = -[B^*(s,b)]_i\{k_{i2}[I^\cdot]_i + k_{fg}([S^\cdot]_i + [P^\cdot]_i)\}V_i$$
$$i = \text{I,II} \quad \text{(A.52b)}$$

$$T_{2_i} = k_{fm}[\text{st}]_i\Sigma_{m=1}^{s}[P^\cdot_m(s-m,b)]_iV_i + k_{tc}\sum_{m=2}^{s}\sum_{n=1}^{m-1}[P^\cdot_n(s-m,b)]_i[S^\cdot_{m-n}]_iV_i + k''_{tc}\sum_{m=1}^{s}[P^\cdot_0(s-m,b)]_i[S^\cdot_m]_iV_i$$
$$i = \text{I,II} \quad \text{(A.52c)}$$

$$T_{3_i} = \frac{k_{tc}}{2}\sum_{b_1=1}^{b-1}\sum_{s_1+m=2}^{s}\sum_{n=1}^{m-1}[P^\cdot_{m-n}(s-s_1,b-b_1)]_i[P^\cdot_n(s_1,b_1)]_iV_i + \sum_{b_1=1}^{b-1}\sum_{s_1+m=2}^{s}k''_{tc}[P^\cdot_m(s-s_1-m,b-b)]_i[P^\cdot_0(s_1,b_1)]_iV_i \quad i = \text{I,II} \quad \text{(A. 52d)}$$

$$T_{4i} = k'_{fm}[\text{St}]_i[P^\cdot_0(s,b)]_iV_i \quad i = \text{I,II} \quad \text{(A.52e)}$$

$$T_{5i} = \frac{k'_{tc}}{2}\sum_{b_1=1}^{b-1}\sum_{s_1=1}^{s}[P^\cdot_0(s-s_1,b-b_1)]_i[P^\cdot_0(s_1,b_1)]_iV_i$$
$$i = \text{I,II} \quad \text{(A.52f)}$$

where (for each phase i), T_{1i} represents the rate of disappearance of the accumulated species P(s,b) by generation of $P^\cdot_0(s,b)$ T_{2i} represents the rate of generation of P(s,b) by grafting of a new T branch of length m onto P($s-m$,b); T_{3i} represents the rate of generation of P(s,b) by linking P($s-s_1-m$,$b-b_1$) and P($s-s_1$,$b-b_1$) with a new H branch of length m; T_{4i} represents the rate of regeneration of P(s,b) by deactivation of primary $P^\cdot_0(s,b)$ radicals; and T_{5i} represents the rate of generation of P(s,b) copolymer by direct crosslinking between $P^\cdot_0(s-s_1,b-b_1)$ and $P^\cdot_0(s_1,b_1)$.

Introducing eqs. (A.8), (A.12), (A.16), (A.33)–(A.38), (A.50), and (A.51) into eq. (A.52a), it results:

$$\frac{d}{dt}\{[P(s,b)]V\} = \sum_i\Bigg\{-\Bigg[R_{Pi}V_i(1-\varphi_i)\Bigg(\tau_i-\gamma_i\tau_{1i}+\beta_i\varphi_i+\frac{\gamma_i\tau_{1i}\varphi_i}{1-\varphi_i}\Bigg)\Bigg]\frac{[B^*(s,b)]_i}{[B^*]_i} + [R_{Pi}V_i(1-\varphi_i)(\beta_i(1-\varphi_i)+2\gamma_i\tau_{1i})] + \Bigg[\frac{R^2_{Pi}V_i\gamma_i^2k''_{tc}}{(k_{Pi}[\text{st}]_i)^2}\Bigg]\frac{[B^*(s,b)]_i}{[B^*]_i} + R_{Pi}V_i(1-\varphi_i)\Bigg(\tau_i-\gamma_i\tau_{1i}+\frac{\gamma_i\tau_{1i}\varphi_i}{1-\varphi_i}\Bigg)\sum_{m=1}^{s}\frac{[B^*(s-m,b)]_i}{[B^*]_i}\alpha_ie^{-\alpha_im} + R_{Pi}V_i\varphi_i(1-\varphi_i)\beta_i\sum_{m=1}^{s}\frac{[B^*(s-m,b)]_i}{[B^*]_i}\alpha_i^2me^{-\alpha_im} + R_{Pi}V_i(1-\varphi_i)\gamma_i\tau_{1i}\times\sum_{b_1=1}^{b-1}\sum_{s_1+m=1}^{s}\frac{[B^*(s-s_1-m,b-b_1)]_i}{[B^*]_i}\times\frac{[B^*(s_1,b_1)]_i}{[B^*]_i}\alpha_ie^{-\alpha_im} + R_{Pi}V_i\times(1-\varphi_i)^2\frac{\beta_i}{2}\sum_{b_1=1}^{b-1}\sum_{s_1+m=1}^{s}\frac{[B^*(s-s_1-m,b-b_1)]_i}{[B^*]_i}\times\frac{[B^*(s_1,b_1)]_i}{[B^*]_i}\times\alpha_i^2me^{-\alpha_im} + \frac{R^2_{Pi}V_i\gamma_i^2k''_{tc}}{2(k_{Pi}[\text{st}]_i)^2}\sum_{b_1=1}^{b-1}\frac{[B^*(s-s_1,b-b_1)]_i}{[B^*]_i}\times\frac{[B^*(s_1,b_1)]_i}{[B^*]_i}\Bigg\}$$
$$s,b = 1,2,3,\ldots i = \text{I,II} \quad \text{(A.53)}$$

The WCLD of the total copolymer is obtained after multiplying each of eqs. (A.53) by the corresponding copolymer molecular weights (sMSt+bMBd), resulting:

$$\frac{d}{dt}G_C(s,b) = \frac{d}{dt}[G_{C_I}(s,b) + G_{C_{II}}(s,b)] = \sum_i\Bigg\{-\Bigg[R_{Pi}V_i(1-\varphi_i)\Bigg(\tau_i-\gamma_i\tau_{1i}+\beta_i\varphi_i+\frac{\gamma_i\tau_{1i}\varphi_i}{1-\varphi_i}\Bigg)\Bigg]\times\frac{[B^*(s,b)]_i}{[B^*]_i}(sM_{St}+bM_{Bd}) + [R_{Pi}V_i(1-\varphi_i)(\beta_i(1-\varphi_i)+2\gamma_i\tau_{1i})] + \Bigg[\frac{R^2_{Pi}V_i\gamma_i^2k''_{tc}}{(k_P[\text{st}]_i)^2}\Bigg]\frac{[B^*(s,b)]_i}{[B^*]_i}(sM_{St}+bM_{Bd}) + R_{Pi}V_i(1-\varphi_i)$$

$$\times\left(\tau_i-\gamma_i\tau_{1i}+\frac{\gamma_i\tau_{1i}\varphi_i}{1-\varphi_i}\right)\sum_{m=1}^{s}\frac{[B^*(s-m,b)]_i}{[B^*]_i}\alpha_i e^{-\alpha_i m}(sM_{St}+bM_{Bd})$$

$$+R_{Pi}V_i\varphi_i(1-\varphi_i)\beta_i\sum_{m=1}^{s}\frac{[B^*(s-m,b)]_i}{[B^*]_i}\alpha_i^2 m e^{-\alpha_i m}(sM_{St}+bM_{Bd})$$

$$+R_{Pi}V_i(1-\varphi_i)\gamma_i\tau_{1i}\sum_{b_1=1}^{b-1}\sum_{s_1+m=1}^{s}\frac{[B^*(s-s_1-m,b-b_1)]_i}{[B^*]_i}\frac{[B^*(s_1,b_1)]_i}{[B^*]_i}$$

$$\times\alpha_i e^{-\alpha_i m}(sM_{St}+bM_{Bd})+R_{Pi}V_i(1-\varphi_i)^2\frac{\beta_i}{2}$$

$$\times\sum_{b_1=1}^{b-1}\sum_{s_1+m=1}^{s}\frac{[B^*(s-s_1-m,b-b_1)]_i}{[B^*]_i}\frac{[B^*(s_1,b_1)]_i}{[B^*]_i}\alpha_i^2 m e^{-\alpha_i m}$$

$$\times(sM_{St}+bM_{Bd})+\frac{R_{Pi}^2V_i\gamma_i^2k''_{tc}}{2(k_p[st]_i)^2}\sum_{b_1=1}^{b-1}\frac{[B^*(s-s_1,b-b_1)]_i}{[B^*]_i}$$

$$\times\frac{[B^*(s_1,b_1)]_i}{[B^*]_i}(sM_{St}+bM_{Bd})\Bigg\}$$

$$s,b=1,2,3,\ldots i=\mathrm{I,II} \quad (A.54)$$

Equation (A.54) indicates that the WCLD of the total copolymer is obtained by integration of the instantaneously-produced WCLD that is generated in each phase. To calculate the cumulative WCLD, eqs. (A.1)–(A.27), (A.33)–(A.38) and (A.54) must be simultaneously solved.

Average molecular weights

The average molecular weights of the free PS and residual PB are calculated in the standard fashion, from their (univariate) WCLDs. Similarly, the average molecular weights of the graft copolymer are calculated from its bivariate WCLD.

References

1. Bucknall, C. B. Toughened Plastics; Applied Science Publishers: London, 1979.
2. Bucknall, C. B. In Polymer Blends; Paul, D. R.; Bucknall, C. B., Eds.; Wiley: New York, 1999; Vol. 2, p 83.
3. Bucknall, C. B.; Karpodinis, A. M.; Zhang, X. C. J Mater Sci 1994, 29, 3377.
4. Fischer, M.; Hellmann, G. P. Macromolecules 1996, 29, 2498.
5. Echte, A.; Haaf, F.; Hambrecht, J. Angew Makromol Chem 1981, 93, 372.
6. Peng, F. M. J Appl Polym Sci 1990, 40, 1289.
7. Soto, G.; Nava, E.; Rosas, M.; Fuenmayor, M.; González, I.; Meira, G.; Oliva, H. J Appl Polym Sci 2003, 92, 1397.
8. Brydon, A.; Burnett, G. M.; Cameron, G. G. J Appl Polym Sci Polym Chem Ed 1973, 11, 3255.
9. Stein, D. J.; Fahrbach, G.; Addler, H. Adv Chem Ser 1975, 142, 148.
10. Fisher, J. P. Angew Chem Int Ed Engl 1973, 12, 428.
11. Gasperowicz, A.; Laskawski, W. J Polym Sci 1976, 14, 2875.
12. Kennedy, J. P.; Delvaux, J. M. Adv Polym Sci 1981, 38, 141.
13. Sardelis, K.; Michelis, H. J.; Allen, G. J Appl Polym Sci 1983, 28, 3255.
14. Solov'eva, A. V.; Bulotova, V. M.; Egorova, E. A.; Kirillova, E. A.; Kuznetsova, S. V. Plasticheskie Massy 1983, 9, 13.
15. Okamoto, Y.; Miyagi, H.; Kakugo, M. Macromolecules 1991, 24, 5639.
16. Oliva, H.; Paricano, G. Polo J Rev Téc Univ Zulia 1993, 6, 43.
17. Huang, N. J.; Sundberg, D. C. J Appl Polym Sci 1994, 35, 5693.
18. Tung, L. H.; Wiley, R. M. J Polym Sci Polym Phys Ed 1973, 11, 1413.
19. Maestrini, C.; Merlotti, M.; Vighi, M.; Malaguti, E. J Mater Sci 1992, 27, 5994.
20. Huang, N. J.; Sundberg, D. C. J Appl Polym Sci 1995, 33, 2551.
21. Estenoz, D. A.; Vega, J. R.; Oliva, H. M.; Meira, G. R. Int J Polym Anal Char 2001, 6, 315.
22. Estenoz, D. A.; Vega, J. R.; Oliva, H. M.; Meira, G. R. Int J Polym Anal Char 2001, 6, 339.
23. Estenoz, D. A.; Vega, J. R.; Oliva, H. M.; Meira, G. R. J Liq Chrom Relat Technol 2002, 25, 2781.
24. Riess, G.; Gaillard, P. Macromol Symp 1983, Vol 17, 221.
25. Oliva, H. Rev Téc Univ Zulia 1993, 16, 67.
26. Brydon, A.; Burnett, G. M.; Cameron, G. G. J Polym Sci Polym Chem Ed 1974, 12, 1011.
27. Ludwico, W. A.; Rosen, S. L. J Appl Polym Sci 1975, 19, 757.
28. Manaresi, V.; Passalacqua, V.; Pilati, F. Polymer 1975, 16, 520.
29. Sundberg, D. C.; Arndt, J.; Tang, M. Y. J Dispersion Sci Technol 1984, 5, 433.
30. Chern, Ch. Sh.; Poehlein, G. W. Chem Eng Commun 1987, 60, 101.
31. Huang, N. J.; Sundberg, D. C. J Appl Polym Sci 1995, 33, 2533.
32. Estenoz, D. A.; Meira, G. R. J Appl Polym Sci 1993, 50, 1081.
33. Estenoz, D. A.; Valdez, E.; Oliva, H. M.; Meira, G. R. J Appl Polym Sci 1996, 59, 861.
34. Estenoz, D. A.; Leal, G. P.; Lopez, Y. R.; Oliva, H. M.; Meira, G. R. J Appl Polym Sci 1996, 62, 917.
35. Estenoz, D. A.; Gómez, N.; Oliva, H. M.; Meira, G. R. AIChE J 1998, 44, 427.
36. Estenoz, D. A.; Gonzalez, I. M.; Oliva, H. M.; Meira, G. R. J Appl Polym Sci 1999, 74, 1950.
37. Schierholz, J. U.; Hellmann, G. P. Polymer 2002, 44, 2005.
38. White, J. L.; Patel, R. D. J Appl Polym Sci 1975, 19, 917.
39. Kruse, R. L. Copolymers, Polyblends, and Composites; American Chemical Society: Washington, DC, 1974; p 141.
40. Johnston, G. J. Polymer 1978, 19, 227.
41. Ludwico, W. A.; Rosen, S. L. J Appl Polym Sci 1976, 14, 2121.
42. García, N.; Meira, G.; Oliva, H. VIII Simposio Latinoamericano de Polímeros 2002, Acapulco (México), 321.
43. Tidhar, M.; Merchuk, J. C.; Sembira, A. N.; Wolf, D. Chem Eng Sci 1986, 41, 457.
44. Jordhamo, G. M.; Manson, J. A.; Sperling, L. H. Polym Eng Sci 1986, 26, 517.
45. Yeo, L. Y.; Matar, O. K.; Perez de Ortiz, E. S.; Hewitt, G. F. Chem Eng Sci 2002, 57, 1069.
46. Friis, N.; Hamielec, A. E. ACS Symposium Series 1976, 24, 82.
47. González, I. M.; Meira, G. R.; Oliva, H. M. J Appl Polym Sci 1996, 59, 1015.
48. Villalobos, M. A.; Hamielec, A. E.; Wood, P. E. J Appl Polym Sci 1991, 42, 629.
49. Yoon, W. J.; Choi, K. Y. Polymer 1992, 33, 4582.
50. Luciani, C.; Díaz de León, R.; Estenoz D.; Morales, G.; Meira, G. IX Simposio Latinoamericano de Polímeros, Valencia (España) 2004, C6–6.